RECENT RESULTS ON BEAM-BEAM EFFECTS IN SPACE CHARGE DOMINATED COLLIDING ION BEAMS AT RHIC*

C. Montag, BNL, Upton, NY 11973, USA

Abstract

To search for the critical point in the QCD phase diagram, RHIC has been colliding gold ions at a variety of beam energies ranging from 2.5 GeV/n to 9.8 GeV/n. During these low energy operations below the regular injection energy, significant lifetime reductions due to the beam-beam interaction in conjunction with large space charge tune shifts have been observed. Extensive simulation studies as well as beam experiments have been performed to understand this phenomenon, leading to improved performance during the 7.3 GeV run in FY2014.

INTRODUCTION

The Relativistic Heavy Ion Collider RHIC was designed to collide beams of fully stripped Au ions at a top energy of 100 GeV/nucleon. To search for the critical point in the QCD phase diagram, center-of-mass energies in the range from 5 to 20 GeV per nucleon pair are required, which extends far below the nominal RHIC injection energy of 9.8 GeV/nucleon. At such low energies, the space charge tune shift becomes significant, and typically exceeds the beam-beam tuneshift by an order of magnitude [1].

When RHIC operated at beam energies of 3.85 and 5.75 GeV/nucleon in 2010, a significant reduction in beam lifetime due to the beam-beam interaction was observed, as illustrated in Figure 1. During that entire physics run, the working point was set at $(Q_x, Q_y) = (28.13, 29.12)$ as the result of a brief tune scan.

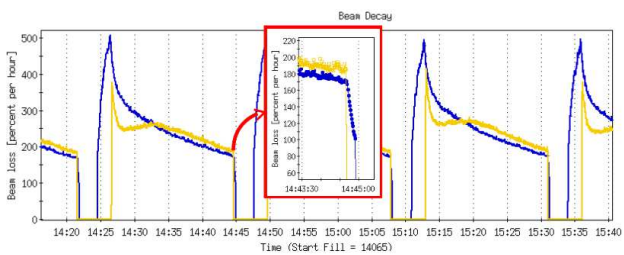

Figure 1: Beam decay rates during several Au beam stores at 5.75 GeVnucleon beam energy. The Blue beam decay rate improves dramatically as soon as the Yellow bean is dumped at the end of each store (see insert). Note that the algorithm to calculate the beam decay rate from the measured beam intensity has a time constant of 20 sec. Hence, the actual drop in instantaneous beam decay is even more dramatic than suggested by the picture.

To gain a better understanding of beam-beam effects in space charge dominated colliding ion beams, extensive simulations have been performed. In the following sections, we describe the simulation methods and present results on emittance growth as well as frequency map analysis and diffusion studies.

* Work supported by Brookhaven Science Associates, LLC under Contract No. DE-AC02-98CH10886 with the U.S. Department of Energy.

TRACKING MODELS

Space charge simulations tend to be very CPU-time consuming due to the frequent recalculations of the particle distributions and associated electro-magnetic fields. However, in the particular problem under study here, we can take advantage of the fact that the evolution of the particle distribution is comparatively slow, as indicated by the experimentally observed beam decay of several hundred percent per hour, which is equivalent to a beam lifetime of tens of minutes. Since typical simulations track particles only over a number of turns that corresponds to seconds in real beamtime, we can therefore assume that the particle distribution remains constant in amplitude space over the course of the simulation. This approach, which is similar to the weak-strong method of beam-beam simulations, significantly speeds up the simulation. In addition, since re-calculating the electro-magnetic fields from the actual particle distribution is avoided, no artificial noise due to the limited number of particles is introduced into the simulation. Furthermore, since the space charge kicks do not depend on the actual distribution of test particles, we can apply methods such as frequency map analysis or action diffusion that require special, non-realistic distributions.

Two different accelerator models are used for tracking, a simplified "toy model", and the realistic RHIC lattice. The simplified model consists of 11 FODO cells. The quadrupoles are modeled as thin lenses, while the dipoles in this "ring" are just drifts, i.e. their bending radius is infinite. 10 of these FODO cells are identical, while in the 11th cell the quadrupole strengths are increased by 3 percent to break the periodicity of the lattice. The phase advance per FODO cell is approximately 108 degrees, depending on the exact working point. In the center of one of the drifts of the 11th cell a beam-beam kick is applied. The drift spaces ("dipoles") are subdivided into 32 slices of equal length each; at the end of each slice a space charge kick is applied according to the local β-functions and the beam emittance, which is assumed to be constant. The tune is adjusted using all quadrupoles simultaneously. The space charge tune shift in this model is set to $\xi_{sc} = -0.05$, while the beam-beam tune shift is set to $\xi_{bb} = -0.003$. In cases without beam-beam interaction, the space charge tune shift is set to $\xi_{sc} = -0.053$; this ensures that the total tune shift is indentical in both cases.

ISBN 978-3-95450-173-1

The large number of defocusing space charge and beam-beam kicks modifies the optics, and therefore the β-functions at each kick location, while the kicks themselves depend on the local RMS beam sizes and therefore the actual β-functions. In a first step, the self-consistent β-functions in the presence of (linearized) space charge and beam-beam kicks are determined. Using this information, in the second step test particles are tracked and the appropriate space charge and beam-beam kicks are applied at each slice, depending on the local RMS beam sizes.

The second approach uses the MADX-SC program to model space charge in the real RHIC lattice. Space charge kicks are applied at each quadrupole, while beam-beam collisions are modeled at IPs 6 and 8. Multipole errors are added to each dipole and each quadrupole based on measurements on a single spare dipole and a single spare quadrupole at a field strength corresponding to 2.5 GeV/nucleon Au ions. Since this model had been benchmarked against dynamic aperture measurements with 5.86 GeV protons, which have the same rigidity and therefore use the same lattice as 2.5 GeV/nucleon Au ions, measured beam parameters for 5.86 GeV protons are used throughout the study. Table 1 lists the relevant beam parameters used in this study.

Table 1: Beam Parameters for the MADX-SC RHIC Tracking Model

beam energy [GeV]	5.86
bunch intensity	$4 \cdot 10^{10}$
transverse rms emittance [mm mrad]	0.16
β^* [m]	10
σ_{IP} [mm]	1.3
RMS bunch length [m]	3.0
space charge tune shift	-0.065
beam-beam tuneshift per IP	-0.005

RESULTS

Most of the tracking studies were performed using the simplified "toy" model. As a first step, a tune scan was performed along a parallel to the coupling resonance, from $(Q_x, Q_y) = (3.09, 3.08)$ to $(3.35, 3.34)$, and the emittance growth rate was determined by tracking 1000 particles over 20000 turns and fitting a straight line to the turn-by-turn 4D emittance data. The number of slices, and therefore space charge kicks, per drift was set to 8, 16, and 32, respectively, to determine the necessary number of slices. This study resulted in the number of slices set to 32 throughout the entire tracking study.

Adding the beam-beam kick leads to an additional breaking of the periodicity of the lattice. To ensure that the observed emittance growth is indeed caused by the nonlinear nature of the beam-beam force and not due to broken periodicity, we compare the results obtained with the nonlinear beam-beam kick with those using only the linearized part of the beam-beam force. As Figure 2 demonstrates, the observed emittance growth is indeed dominated by the nonlinearity of the beam-beam kick. With the nonlinear beam-beam kick added, tunes close to the integer exhibit the smallest emittance growth, while the emittance growth rate increases almost monotonically with the distance from the integer. Without the beam-beam kick, no emittance growth is observed within the error bars of the linear fit at any working point during the scan, which is in qualitative agreement with experimental observations of beam lifetime.

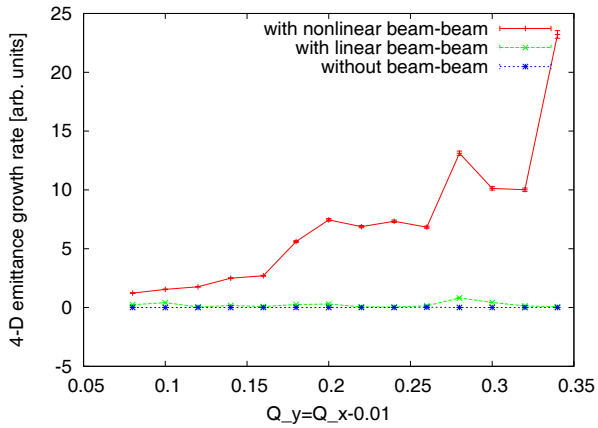

Figure 2: Emittance growth rates during a tune scan with a nonlinear (red) and a linearized (green) beam-beam kick in addition to the nonlinear space charge kicks. The blue line corresponds to the case without any beam-beam interaction.

To provide a better understanding of the underlying mechanism causing the emittance growth in the presence of the beam-beam interaction, the method of frequency map analysis was used. For this purpose, a single test particle was tracked over 1024 turns, and the tune for the first and last 512 turns was determined to high precision using an interpolated FFT technique [2]. As Figure 3 shows for the FY2010 fractional working point $(Q_x, Q_y) = (.13, .12)$, the presence of the beam-beam interaction results in a significant enhancement of tune diffusion, especially along the coupling resonance $Q_x = Q_y$. A similar picture is obtained at the near-integer working point $(Q_x, Q_y) = (.09, .08)$, as shown in Figure 4.

Comparing these two working points in amplitude space yields similar results, Figure 5, with the near-integer working point showing slightly higher tune diffusion at smaller amplitudes. This is surprising insofar as the tune scan (Figure 2) indicates a significantly smaller emittance growth at these tunes.

All results presented so far are obtained in a purely linear lattice, with the space charge and beam-beam forces being the only non-linearities. This limitation is overcome by tracking in the realistic RHIC lattice with its known nonlinearities, both from lattice sextupoles and multipole errors. Comparing tune diffusion in the RHIC lattice for the FY2010 working point, $(Q_x, Q_y) = (.13, .12)$, and the near-integer working point $(Q_x, Q_y) = (.095, .085)$ shows higher tune diffusion at smaller amplitudes at the near-integer working point than at $(.13, .12)$, see Figure 6. This is in stark contrast to experimental results obtained during beam experiments in previous years as well as during FY2014 which showed

ISBN 978-3-95450-173-1

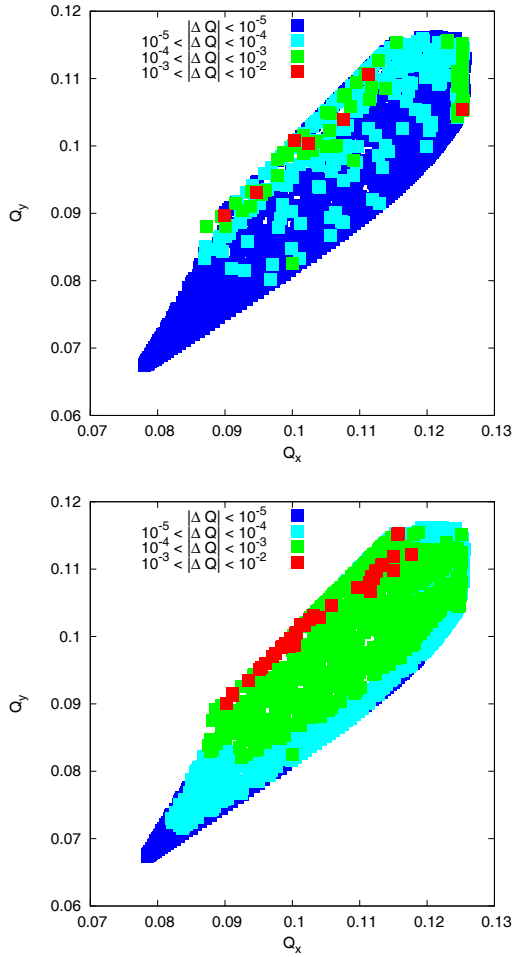

Figure 3: Tune footprints in the "toy" model without (top) and with (bottom) beam-beam interaction, for a working point of $(Q_x, Q_y) = (.13, .12)$.

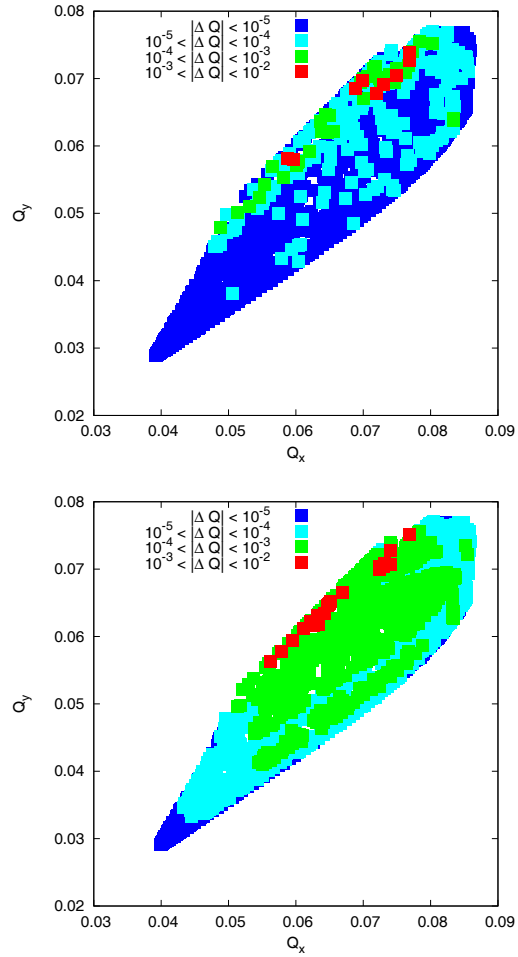

Figure 4: Tune footprints in the "toy" model without (top) and with (bottom) beam-beam interaction, for a working point of $(Q_x, Q_y) = (.09, .08)$.

improved beam lifetime in collisions at the near-integer working point [3, 4]. Dynamic aperture simulations qualitatively agree with this experimental result as well.

The fact that those areas with enhanced diffusion correspond to particles on or near the linear coupling resonance $(Q_x = Q_y)$ leads to the suspicion that at least on this particular resonance tune diffusion does not necessarily indicate amplitude diffusion. To prove this theory, we perform a tune scan on the linear coupling resonance and record the emittance growth as a function of tune, using our "toy" model. As Figure 7 shows, there is still no emittance growth without beam-beam interaction.

If we now perform a frequency map analysis at the working point $(Q_x, Q_y) = (.08, .08)$, we notice very strong tune diffusion even at small amplitudes, as depicted in Figure 8. The fact that this tune diffusion does not translate into emittance growth proves that frequency map analysis is misleading when studying beam-beam effects in space charge dominated ion beams. Instead of tune diffusion, we therefore study amplitude diffusion.

We define the amplitude diffusion coefficient as [5]

$$D(J_x, J_y) = \lim_{N\to\infty} \frac{\sigma^2_{J_x}(N) + \sigma^2_{J_y}(N)}{N}, \quad (1)$$

where N denotes the number of turns and $\sigma_{J_x}(N), \sigma_{J_y}(N)$ the rms action spread at turn N of a set of particles launched at identical horizontal and vertical action values J_x, J_y in phase space.

At regular intervals in the (J_x, J_y) space, we launch 100 particles of equal action $J_{x,i}$, $J_{y,i}$ in phase space and track them over 10000 turns. After each turn N, we calculate the RMS action spread

$$J_{\mathrm{RMS}}(N)^2 = \langle (J_i(N) - \langle J(N)\rangle)^2\rangle \quad (2)$$

$$= \langle (J_{x,i}(N) - \langle J_x(N)\rangle)^2 + (J_{y,i}(N) - \langle J_y(N)\rangle)^2\rangle \quad (3)$$

and perform a linear fit

$$J_{\mathrm{RMS}}(N)^2 = a + bN \quad (4)$$

ISBN 978-3-95450-173-1

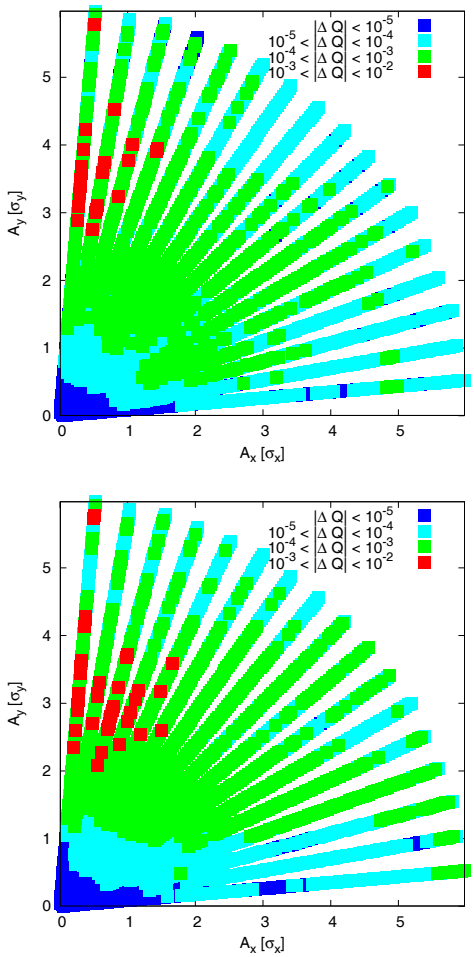

Figure 5: Tune diffusion at two working points, in amplitude space. Top: $(Q_x, Q_y) = (.09, .08)$. Bottom: $(Q_x, Q_y) = (.13, .12)$.

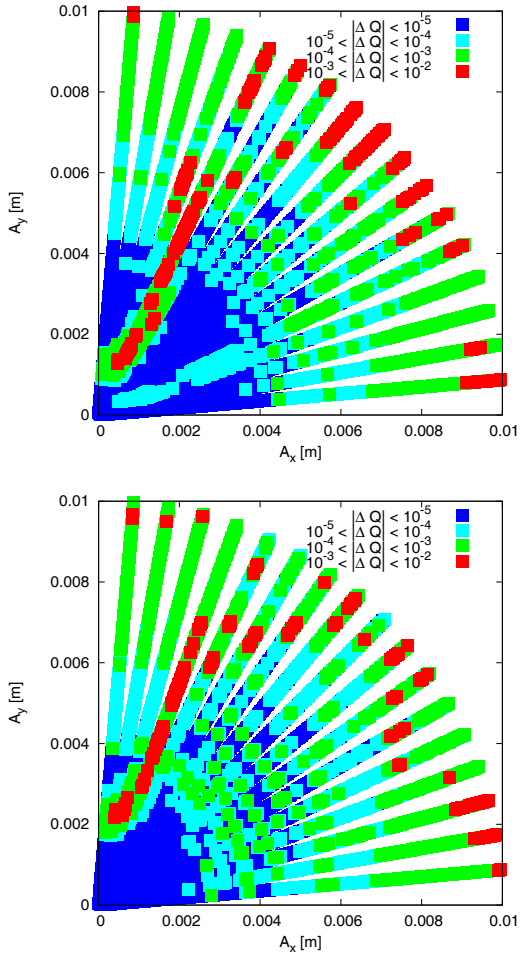

Figure 6: Tune diffusion in the RHIC lattice with beam-beam interaction, in amplitude space. Top: $(Q_x, Q_y) = (28.095, 30.085)$. Bottom: $(Q_x, Q_y) = (28.13, 30.12)$.

to determine the diffusion coefficient

$$D(J) = \lim_{N\to\infty} \frac{\sigma_J^2(N)}{N} = b. \quad (5)$$

As Figure 9 shows, the diffusion coefficient $D(J)$ at amplitudes below 4σ is larger the further away from the integer the working point is chosen. This result is consistent with the emittance growth data obtained using the same tracking model, shown in Figure 2. Since only 1000 particles were tracked to obtain those emittance growth data, amplitudes beyond 4σ are irrelevant because the probability of any one of those 1000 particles being launched at such large amplitudes is extremely small.

DISCUSSION

Simulation studies in the "toy" model show that emittance growth rates due to the beam-beam interaction in space charge dominated ion beams increase with the distance of the working point from the integer resonance, which is in agreement with lifetime observations in RHIC. However, this observation is not supported by frequency map analysis

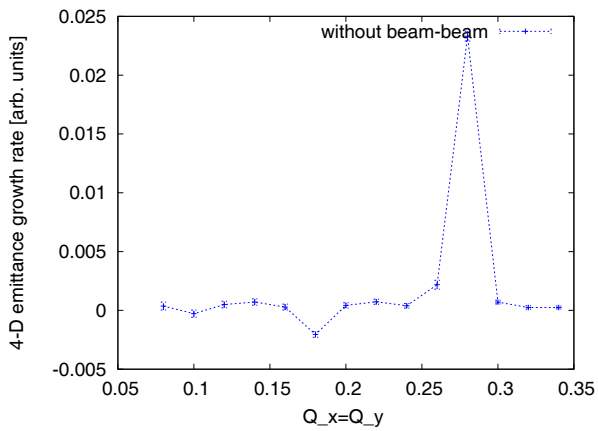

Figure 7: Emittance growth rates without beam-beam interaction on the coupling resonance as a function of tune.

in the same tracking model, thus indicating that tune diffusion studies are not suitable for an understanding of the underlying dynamics. Amlitude diffusion simulations, on the other hand, agree with emittance growth simulations and experimental observations of beam lifetime.

ISBN 978-3-95450-173-1

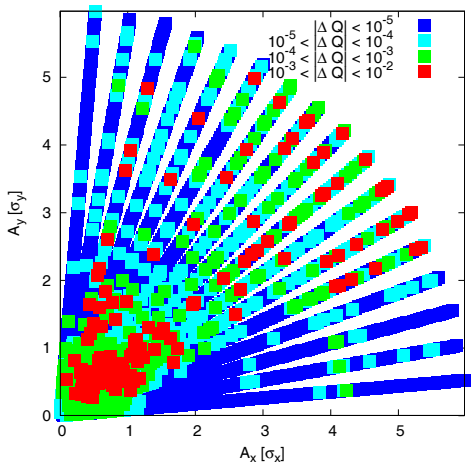

Figure 8: Tune diffusion on the coupling resonance without beam-beam interaction, in amplitude space. $(Q_x, Q_y) = (.08, .08)$.

REFERENCES

[1] A. Fedotov et al., "Beam Lifetime and Limitations during Low-energy RHIC Operation", Proc. PAC'11

[2] A. Bazzani et al., Part. Accel. **52**, 147 (1996)

[3] C. Montag and A. Fedotov, "Beam-Beam Effects in Space Charge Dominated Ion Beams" Proc. Beam-Beam 2013, CERN-2014-004

[4] C. Montag et al., "RHIC Performance During the 7.5 GeV Low Energy Run in FY 2014" Proc. IPAC 2014

[5] N. Abreu et al., C-A/AP/346

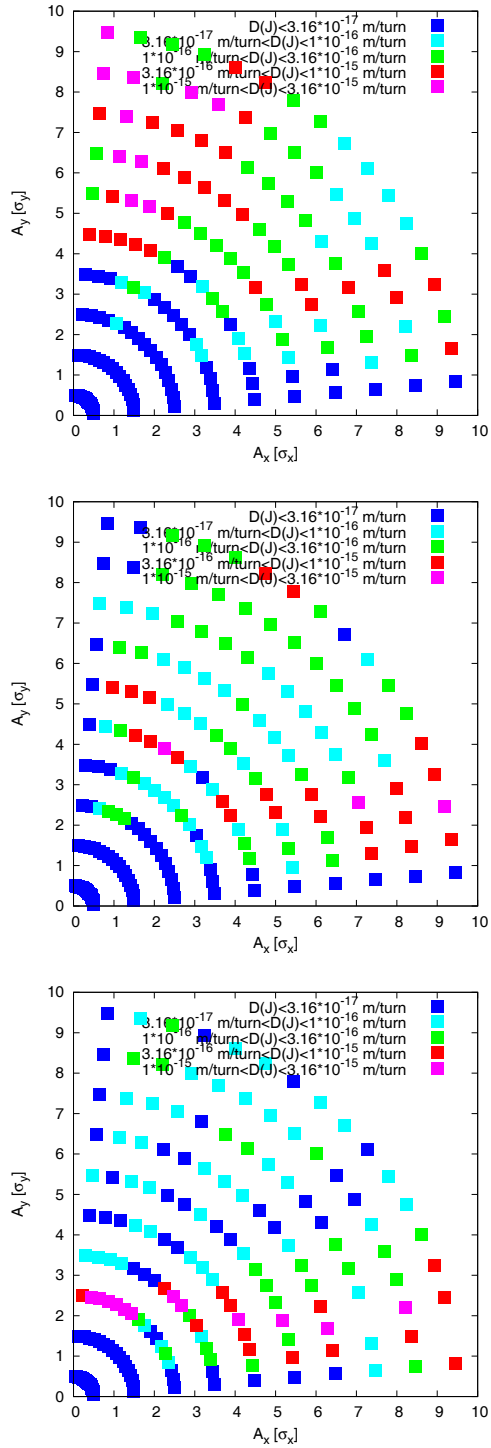

Figure 9: Amplitude diffusion with beam-beam interaction in the "toy" model at the near-integer working point $(Q_x, Q_y) = (.095/.085)$ (top), the FY2010 working point $(.13, .12)$ (center), and the RHIC high energy ion working point $(.23, .22)$ (bottom).

ISBN 978-3-95450-173-1